2021 43rd Annual International Conference of the
IEEE Engineering in Medicine & Biology Society (EMBC)
Oct 31 - Nov 4, 2021. Virtual Conference

2021 43rd Annual International Conference of the IEEE Engineering in Medicine & Biology Society (EMBC) | 978-1-7281-1179-7/21/$31.00 ©2021 IEEE | DOI: 10.1109/EMBC46164.2021.9630735

Proof-of-principle Experiment on 24 GHz Medical Radar for Non-contact Vital Signs Measurement

Hoang Thi Yen, Masaki Kurosawa, Tetsuo Kirimoto, *Senior Member, IEEE*, Keisuke Edanami and Guanghao Sun, *Senior Member, IEEE*

***Abstract*—Medical radar for non-contact vital signs measurement exhibits great potential in both clinical and home healthcare settings. Especially during the corona virus spreading time, non-contact sensing more clearly shows the advantages. Many previous studies have concentrated on medical radar-based healthcare applications, but pay less attention to the working principles. A clear understanding of medical radars at both the mathematical and physical levels is critically important for developing application-specific signal processing algorithms. Therefore, this study aims to re-define the operating principle of radar, and a proof-of-principle experiment was performed on both actuator and human subjects using 24 GHz Doppler radar system. Experimental results indicate that there is a difference in the radar output signals between the two cases, where the displacement is greater than and less than half of the wavelength. For the former situation, the displacement $x = n.\lambda/2$ $(n \geq 1)$, one peak of radar signals corresponds to n peaks of baseband signals. By contrast, for the latter situation, the displacement $x < \lambda/2$, one peak of radar signals corresponds to one peak of baseband signals. Strikingly, with human measurement on the dorsal side, the the number of respiration peaks are seen from the radar raw signals.**

I. Introduction

Medical radar for non-contact vital signs measurement is one of the most promising solutions in both clinical and home healthcare settings. For instance, a radar-based non-contact system becomes more important in situations where the skin is damaged, which cannot attach an electrode to the patient's skin to measure the electrocardiography signal (ECG) and in the absence of skin damage, patient discomfort remains [1], [2]. Medical radar can remotely obtain heartbeat and respiration rate at a distance from a subject, but the signals obtained by using the radar do not show clear peaks like those in the ECG because of the operating characteristics of the radar. Many previous works have used radar to collect and process signals to extract vital signs information. From the perspective of digital signal processing, the time domain peak-detection algorithm has been applied for the acquisition of respiration and heart signals [3]–[5], to create the infection screening systems in diagnosing influenza [6]. An ultra-wide band (UWB) radar-based system was developed to cancel harmonics as well as interference [7]–[9]. Moreover, recent works have used radar output to detect heartbeat using neural networks [4], [10]. However, there are few previous works that explain in detail why radar channel signals can carry information on the tiny movement of the human chest corresponding to cardiac and pulmonary peaks [11].

Hence, in this study, we restate the principle of the I and Q channels on the 24 GHz Doppler radar and explain why the received wave after the human reflection contains information on chest movement. In addition, the experiments show that human measurement from dorsal side can give the information of respiration rate, which does not need to demodulate. Respiratory and heart movements can be detected by 24 GHz Doppler radar and are concentrated in the human chest and heart lie. The chest surface motion associated with respiration varies from 4 to 12 mm depending on individual physiology [12], whereas the chest wall motion due to heartbeat has an average of 0.6 mm [13]. The radar system can simultaneously measure chest surface motion caused by respiration and heart movement. We first explained the principle of radar for vital measurement at the mathematical level based on physiological motion. In this work, we designed a proof-of-principle experiment using 24 GHz Doppler radar. To obtain the Doppler frequency in the radar output, the movement needs to move at least more than 1/2 the wavelength (λ) of the transmitted frequency. In the case of a 24 GHz sensor, the half of wavelength is approximately 6.2 mm. ($f = 24GHz, \lambda = 12.4mm, \lambda/2 = 6.2mm$). Therefore, the experiments were performed using an actuator and a human subject with different depth of breathing. With the plate experiment, the depth of plate movement can be easily change by setting the plate control program from the computer. In the human experiment, the subject was asked to breathe normally and deeply, so that the chest wall produced a displacement smaller than $\lambda/2$ and greater than $\lambda/2$, respectively. With different movement

*Research supported by JSPS Grant-in-Aid for Scientific Research (B) No. 19H02385

Hoang Thi Yen, Masaki Kurosawa, Tetsuo Kirimoto, Keisuke Edanami and Guanghao Sun, are with The University of Electro-Communications, 1-5-1 Chofugaoka, Chofu, Tokyo 182-8585, Japan (phone: +81-42-443-5412; e-mail: yen@secure.ee.uec.ac.jp; guanghao.sun@uec.ac.jp).

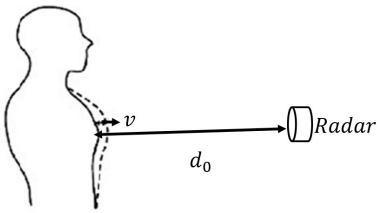

Fig. 1. System of radar for non-contact vital signs measurement

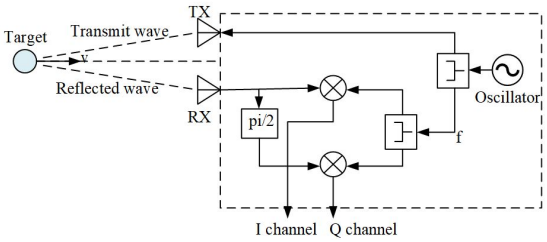

Fig. 2. Structure of a 24 GHz radar

depths, the relationship between the peaks number of base band signal and the peaks number of the raw radar signal will be different.

The remainder of this paper is organized as follows. Section II presents the principle of continuous-wave (CW) Doppler radar in mathematical detail. The proof-of-principle experiments on 24 GHz radar for actuator and human subjects are demonstrated in Section III. Finally, some discussions and conclusions are presented in Section IV.

II. Principle of CW doppler radar with Vital signs

Suppose that a radar system emits the signal, and the transmitted signal hits the chest region in the body, chest wall moves with velocity v, as shown in Fig. 1. This section will analyze in detail the inhalation process as the chest moves towards the radar. Similar principles are applicable to the exhalation process.

Let d_0 refer to the distance from radar to the object at time t_0 (time reference) [14]. Then the distance to the chest at any time t is

$$d(t) \;=\; d_0 \;-\; v(t - t_0) \tag{1}$$

The signal received by the radar is then given as

$$x_r(t) \;=\; x(t - \psi(t)) \tag{2}$$

where $x(t)$ is the transmitted signal, and

$$\psi(t) = \frac{2.d(t)}{c} = \frac{2}{c}\left(d_0 - vt + vt_0\right) \tag{3}$$

Substituting Eq. (3) into Eq. (2), and collecting the terms yields

$$\begin{aligned} x_r(t) \;&=\; x\left[t - \tfrac{2}{c}\left(d_0 \;-\; vt + vt_0\right)\right] \\ &=\; x\left(t - \tfrac{2d_0}{c} + \tfrac{2vt}{c} - \tfrac{2vt_0}{c}\right) \end{aligned} \tag{4}$$

Since the transmitted signal can be modeled as a cosine harmonic motion as

$$T(t) \;=\; A.\cos\left(2\pi f t\right) \tag{5}$$

Then, the received signal can be written according to Eq.(4)

$$R(t) \;=\; A.\cos\left(2\pi f t - \frac{4\pi d_0}{\lambda} + \frac{4\pi s(t)}{\lambda} - \theta\right) \tag{6}$$

where $s(t) = v.t$ and $\theta = (4\pi v t_0)/\lambda$.

The structure of the CW Doppler radar (New Japan Radio, NJR4262) is presented in Fig. 2. The received signal is combined with the transmitted signal through a multiplier. This means that the two cosine functions in Eq. (5) and Eq. (6) are multiplied. Then, a high-frequency signal at twice the transmitted frequency and baseband signal are obtained. Using the filter to obtain the baseband signal, the I channel signal is obtained as follows

$$B_I(t) \;=\; A_r.\cos\left(\frac{4\pi s(t)}{\lambda} \;-\; \frac{4\pi d_0}{\lambda} - \theta\right) \tag{7}$$

To receive the Q-channel signal, the received signal is delayed by $\pi/2$, and then multiplied by the transmitted signal. Using the filter to obtain the baseband signal, the Q channel signal is obtained as follows

$$B_Q(t) \;=\; A_r.\cos\left(\frac{4\pi s(t)}{\lambda} \;-\; \frac{4\pi d_0}{\lambda} - \theta - \frac{\pi}{2}\right) \tag{8}$$

In the exhalation process (chest wall moves leaving the radar), (1) can be re-written as

$$d(t) \;=\; d_0 \;+\; v(t - t_0) \tag{9}$$

and (6) becomes

$$R(t) \;=\; A.\cos\left(2\pi f t - \frac{4\pi d_0}{\lambda} - \frac{4\pi s(t)}{\lambda} + \theta\right) \tag{10}$$

Applying the principle of operation shown in Fig. 2, the baseband signals of the I and Q channels in the exhalation process are obtained, respectively, as follows

$$B_I(t) \;=\; A_r.\cos\left(\frac{4\pi s(t)}{\lambda} \;+\; \frac{4\pi d_0}{\lambda} - \theta\right) \tag{11}$$

$$B_Q(t) \;=\; A_r.\cos\left(\frac{4\pi s(t)}{\lambda} \;+\; \frac{4\pi d_0}{\lambda} - \theta + \frac{\pi}{2}\right) \tag{12}$$

From Eqs. (7) and (8), it can be observed that when the target moves toward the radar, the I channel signal is always

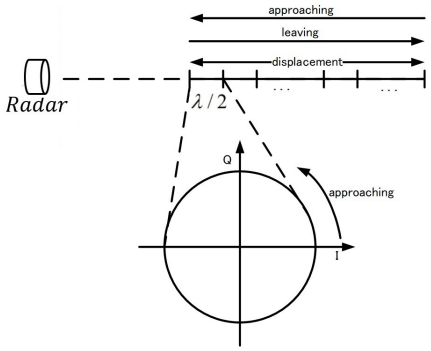

Fig. 3. Principle of radar demodulation

$\pi/2$ earlier than the Q channel signal. In addition, from Eq. (11) and Eq. (12) when the target moves leaving radar, the I channel signal is $\pi/2$ later than the Q channel signal. Rewrite expression (8) as follows

$$B_Q(t) = A_r.\sin\left(\frac{4\pi s(t)}{\lambda} - \frac{4\pi d_0}{\lambda} - \theta\right) \quad (13)$$

Then, dividing the corresponding sides of (13) by (7), the equation can be inferred as

$$\frac{4\pi s(t)}{\lambda} = \arctan\left(\frac{B_Q(t)}{B_I(t)}\right) + \frac{4\pi d_0}{\lambda} + \theta \quad (14)$$

Thus, s(t) has a linear relationship with $\arctan\angle(B_Q(t), B_I(t))$ when the wavelength is fixed.

$$s(t) = \frac{\lambda}{4\pi}.\arctan\left(\frac{B_Q(t)}{B_I(t)}\right) + d_0 + \frac{\lambda}{4\pi}.\theta \quad (15)$$

From Eq. (15), we suppose $s_0 = d_0 + (\lambda.\theta/4\pi)$ is the starting point, if we call x as the displacement and $\alpha = \arctan\angle(B_Q(t), B_I(t))$, x can be written as

$$x = \frac{\lambda}{4\pi}.\alpha \quad (16)$$

Substituting $\alpha = 2\pi$ into (16), we obtain $x = \lambda/2$. It means that displacement is $x = \lambda/2$ corresponding to a circle, and furthermore, when $x = n.(\lambda/2)$ then $\alpha = n.2\pi$ as shown in Fig. 3. We will discuss further details in the next section.

III. PROOF-OF-PRINCIPLE EXPERIMENT ON 24 GHZ MEDICAL RADAR FOR ACTUATORS AND HUMAN SUBJECTS

In this section, the experiments are conducted as follows (Fig. 4). A 24 GHz radar provides I and Q channel signals. A laser device next to the radar is used to measure the distance from radar to the object, as the reference signal, when the object approaches the laser, the voltage will go up and vice versa, and an ADC sampling at 100 Hz. In addition, we

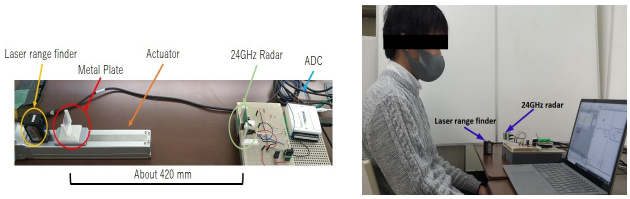

(a) Plate movement (b) Chest movement

Fig. 4. Arrangement of equipment in the experiment measuring the plate and chest movement using 24 GHz radar

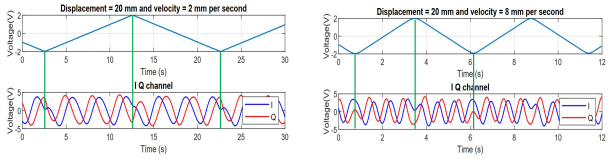

(a) displacement=20 mm and velocity=2 mm/s (b) displacement=20 mm and velocity=8 mm/s

Fig. 5. Radar output and reference signal of plate movement with displacement=20 mm and different velocities, (a) 2 mm/s and (b) 8 mm/s

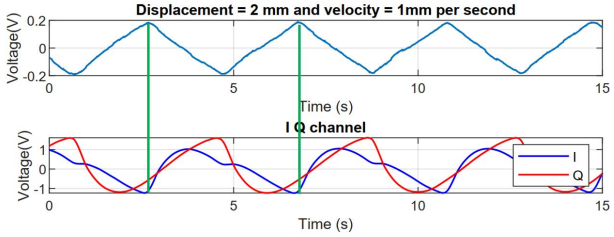

Fig. 6. Radar output and reference signal of plate movement with displacement=2 mm and velocity=1 mm/s, show balanced signals

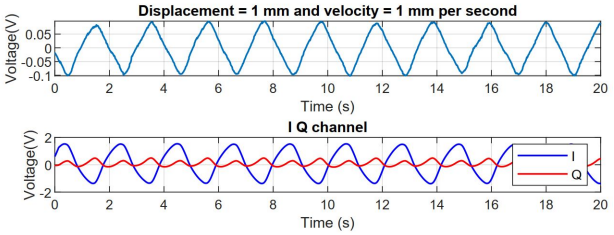

Fig. 7. Radar output and reference signal of plate movement with displacement=1 mm and velocity=1 mm/s, show imbalanced signals

have a PC with an actuator control program that induces the movement of the metal plate and a program that receives data from radar and laser.

We performed the experiment with a metal plate first, so that the displacement in experiment could be precisely controlled by employing an actuator controlled by the PC.

Figures 5–7 present the experiments with metal plates movement. These figures illustrate that when the velocity of movement increases, the Doppler frequency also increases, and the I channel moves $\pi/2$ ahead while approaching, and vice versa when leaving. Moreover, from Figs. 5a and 5b, it can be seen that, for displacement $x = 20mm \simeq 3.2\,\lambda/2$,

we obtain 3.2 IQ peaks for once approaching or leaving for different velocities. Looking back at Eq. (16), we can see that this displacement corresponds to 3.2 circles for once approaching or leaving. Then, the IQ signal frequency will be 6.4 times the plate's frequency.

In the situation of displacement $x < \lambda/2$, the frequency of the IQ signal is equal to that of the object, as shown in Fig. 6. However, in this case, one problem we need to face is the imbalance between two channel amplitudes, as shown in Fig. 7.

This imbalance problem can be solved by choosing the optimal distance from the radar to the object. On the unit circle in Fig. 3, the best balance occurs when the motion goes around the bisector position of the four quadrants.

Figures 8–11 show the explorations with human signal measurement. The person in this experiment is a man from our laboratory, male, healthy, 60kg weight and 170cm tall. Fig. 8 and Fig.9 are the signals when measure from the front side of chest. The man performed deep inhalation and exhalation, causing the chest movement to be larger than $\lambda/2$, is demonstrated in Fig. 8, the frequency of the IQ signal obtained will be greater than the respiration rate. In this case, it is necessary to perform demodulation in order to obtain the breathing rate. As the person breathes normally, the experimental result is illustrated in Fig. 9, and the chest displacement is now shorter than $\lambda/2$. Therefore, the frequency of the IQ signal is equal to breathing rate. On the hand of displacement smaller than $\lambda/2$, imbalance needs to be resolved by appointing the distance from the radar to the human chest. Figs. 10 and 11 are obtained from the back side of the person, but different distances from the radar. Imbalanced and balanced signals are shown in the former and latter figure, respectively.

IV. DISCUSSION AND CONCLUSION

Recently, many research works focus on processing the output signal of radar. Many researchers are eager to find a document with a fundamental analysis of the radar output signal. [2] mentioned radar signal characteristics but has not given mathematical expressions. [4], [9], [10] used radar output expressions corresponding to equation (11), (12) in this paper, but many readers will not understand why there are two expressions. Therefore, this paper has analyzed the very basic steps on the principle of operation of the radar to get the output signal as (11), (12). Furthermore, the paper gave a detailed explanation to get Eq (16) which is the key formula for drawing conclusions about displacements greater than or less than half of wavelength.

Paper [4] acknowledged detecting heartbeat peaks from radar signals, presented a 1:1 correspondence between radar signal peaks and R peaks of ECG. This correspondence can be obtained because the chest movement due to heart beat

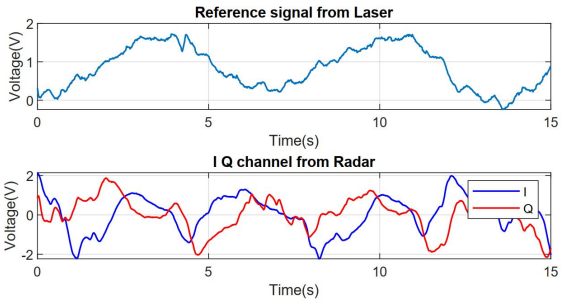

Fig. 8. Radar output and reference signal of deep breath, from front side chest

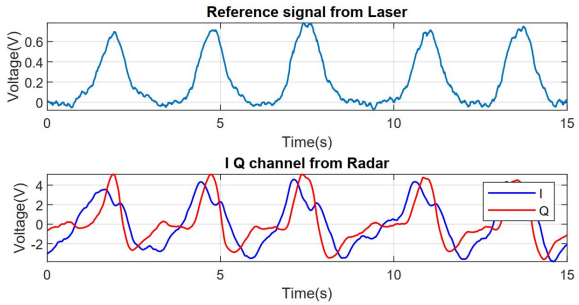

Fig. 9. Radar output and reference signal of normal breath, from front side chest

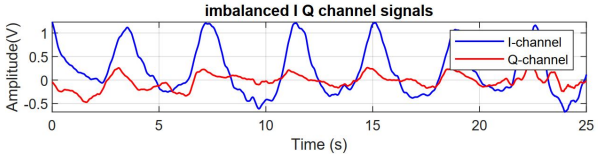

Fig. 10. Imbalanced radar output from back side of human subject

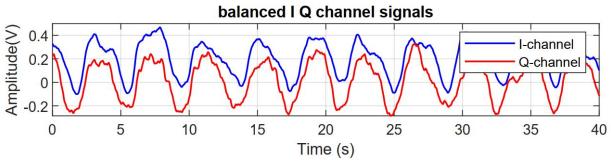

Fig. 11. Balanced radar output from back side of human subject

is smaller than $\lambda/2$. In this case, the IQ signals do not show Doppler frequency information, but the number of IQ peaks caused by the heartbeat and ECG peaks are equal.

From the analysis and experiments above, we can draw some conclusions. In case of displacement larger than half of wavelength, the relationship between frequencies of IQ signals and object does not depend on velocity of object, only depend on the magnitude of displacement, in detail, if $x = n\lambda/2 (n \geq 1)$, frequency of IQ signals equal to n times of object movement frequency. In addition, the signals are balanced between the two channels. In the case of a displacement smaller than half of the wavelength, the frequency of the IQ signals is equal to the object movement frequency. Furthermore, the signals are imbalanced between the two channels. In order to obtain balanced signals, the distance from the radar to the object needs to be chosen. In

addition to this, for vital signs, the measurement from the front side can get displacement larger or smaller than $\lambda/2$, depending on how much of the person's chest dilation when breathing. However, the displacement is always smaller than $\lambda/2$ from the back-side measurement [15], so we can see the respiration rate from raw radar output signals. With note that these conclusions are only evident for good signals which are signals without body random movement.

In conclusion, we illustrated a clear explanation of the principle of the two-channel radar at 24 GHz. The principle was clarified by the plate measurement and human subjects' vital signs experiment. This study provides a detailed explanation for understanding radar signals, which is crucial for further studies, in the tendency of using the non-contact method for patient.

REFERENCES

[1] G. Sun, Y. Tanaka, K. Kiyono, K. Hashimoto, B. Takase, H. Liu, T. Kirimoto, and T. Matsui, "Non-contact monitoring of heart rate variability using medical radar for the evaluation of dynamic changes in autonomic nervous activity during a head-up tilt test," *Journal of Medical Engineering & Technology*, vol. 43, no. 7, pp. 411–417, 2019.

[2] X. Hui and E. C. Kan, "Monitoring vital signs over multiplexed radio by near-field coherent sensing," *Nature Electronics*, vol. 1, no. 1, pp. 74–78, 2018.

[3] J.-Y. Kim, J.-H. Park, S.-Y. Jang, and J.-R. Yang, "Peak detection algorithm for vital sign detection using doppler radar sensors," *Sensors*, vol. 19, no. 7, p. 1575, 2019.

[4] N. Malešević, V. Petrović, M. Belić, C. Antfolk, V. Mihajlović, and M. Janković, "Contactless real-time heartbeat detection via 24 ghz continuous-wave doppler radar using artificial neural networks," *Sensors*, vol. 20, no. 8, p. 2351, 2020.

[5] W.-K. Liu, H.-P. Fu, and Z.-K. Yang, "A doppler radar vital sign detection system using concurrent dual-band hybrid down conversion architecture," *IEICE Electronics Express*, pp. 16–20 190 665, 2019.

[6] G. Sun, Y. Hakozaki, S. Abe, O. Takei, and T. Matsui, "A neural network-based infection screening system that uses vital signs and percutaneous oxygen saturation for rapid screening of patients with influenza," *Health*, vol. 2013, 2013.

[7] A. Lazaro, D. Girbau, and R. Villarino, "Analysis of vital signs monitoring using an ir-uwb radar," *Progress In Electromagnetics Research*, vol. 100, pp. 265–284, 2010.

[8] M. Leib, W. Menzel, B. Schleicher, and H. Schumacher, "Vital signs monitoring with a uwb radar based on a correlation receiver," in *Proceedings of the Fourth European Conference on Antennas and Propagation*. IEEE, 2010, pp. 1–5.

[9] Z. Yu, D. Zhao, and Z. Zhang, "Doppler radar vital signs detection method based on higher order cyclostationary," *Sensors*, vol. 18, no. 1, p. 47, 2018.

[10] S. Wu, T. Sakamoto, K. Oishi, T. Sato, K. Inoue, T. Fukuda, K. Mizutani, and H. Sakai, "Person-specific heart rate estimation with ultra-wideband radar using convolutional neural networks," *IEEE Access*, vol. 7, pp. 168 484–168 494, 2019.

[11] Ø. Aardal, Y. Paichard, S. Brovoll, T. Berger, T. S. Lande, and S.-E. Hamran, "Physical working principles of medical radar," *IEEE Transactions on Biomedical Engineering*, vol. 60, no. 4, pp. 1142–1149, 2012.

[12] A. De Groote, M. Wantier, G. Chéron, M. Estenne, and M. Paiva, "Chest wall motion during tidal breathing," *Journal of Applied Physiology*, vol. 83, no. 5, pp. 1531–1537, 1997.

[13] O. Boric-Lubecke, V. M. Lubecke, A. D. Droitcour, B.-K. Park, and A. Singh, *Doppler radar physiological sensing*. Wiley Online Library, 2016.

[14] B. R. Mahafza and A. Elsherbeni, *MATLAB simulations for radar systems design*. CRC press, 2003.

[15] F. Li, M. Valero, H. Shahriar, R. A. Khan, and S. I. Ahamed, "Wi-covid: A covid-19 symptom detection and patient monitoring framework using wifi," *Smart Health*, vol. 19, p. 100147, 2021.